PHYSICAL REVIEW E **74**, 051708 (2006)

Dielectric study on the shear-induced structural changes in the nematic and the smectic-*A* phases of 4-n-octyl-4′-cyanobiphenyl (8CB)

K. Negita, M. Inoue, and S. Kondo
Department of Chemistry, Faculty of Science, Fukuoka University, Nanakuma 8-19-1, Jonan-ku, Fukuoka 814-0180, Japan

(Received 17 May 2006; published 22 November 2006)

Dielectric measurements under steady shear flow are made to clarify the shear induced structural changes in the nematic (N) and the smectic-A (S_A) phases of 4-n-octyl-4′-cyanobiphenyl (8CB). In the N phase, the temperature dependence of the dielectric permittivity shows a characteristic behavior, which can be consistently interpreted based on the shear-induced structures suggested by x-ray scattering; flow alignment of the director and some dynamical structures characterized by different precessional motions of the director. For the shear-induced structural change in the S_A phase, it is suggested that undulation instability would play an important role.

DOI: 10.1103/PhysRevE.74.051708 PACS number(s): 77.84.Nh, 83.80.Xz, 47.57.Lj, 83.50.Ax

I. INTRODUCTION

The liquid crystals are characterized by the orientational and positional orders of the molecules, and depending on these orders a variety of phases are realized [1,2]. Of various interesting properties of the liquid crystals, the effect of the shear flow is characteristic of the liquid crystals; the shear flow easily modifies the structures of the liquid crystals as well as the electric and magnetic fields. In the case of the nematic (N) phase, a steady shear flow induces an alignment of the director, a unit vector specifying the averaged direction of the liquid crystalline molecules, near the flow direction [1–8]. Such a behavior has been well studied experimentally [3,4] and has been understood in terms of the Leslie-Ericksen theory [5–8]; if the Leslie coefficients α_2 and α_3 satisfy a condition of $\alpha_2/\alpha_3>0$, a flow alignment occurs with the orientational angle θ given by $\tan\theta=(\alpha_2/\alpha_3)^{1/2}$. Such a flow alignment has been observed in the whole temperature region of the N phase if the materials have a phase sequence of crystal (Cry)-nematic (N)-isotropic liquid (I) such as 4-n-pentyl-4′-cyanobiphenyl (5CB) [4]. While in materials having smectic-A (S_A) phase below the N phase, a significant change in the shear-induced structure occurs due to the development of the smectic order. In the case of 8CB, which has a phase sequence of Cry-S_A-N-I, it is suggested from the x-ray scattering experiments that some dynamical structures are induced by a steady shear flow in the N and S_A phases [9,10]. To specify these shear-induced structures in the N phase, three fundamental structures under a shear flow along the y axis are depicted in Fig. 1; a, b, and c structures having director orientations along x, y, and z axes, respectively. The Miesowicz viscosities η_a, η_b, and η_c correspond to those for a, b, and c structures, and similarly we use ε'_a, ε'_b, and ε'_c as the dielectric permittivities along the z axis for a, b, and c structures, respectively. In the S_A phase, additional layering is formed with its normal parallel to the director orientation. To distinguish these from those in N phase, notations a'', b'', and c'' will be used for the fundamental structures in the S_A phase. Using these notations, the shear-induced structures in the N and S_A phases of 8CB are summarized as follows. In the temperature region just below the N-I transition point, a flow alignment of the director (b' structure) occurs with its direction near the flow direction (y axis). Below this temperature region, α_2/α_3 becomes negative [9–11] to make the flow alignment of the director impossible, leading to a-b, a_m, a_s, $a(b)$, and a_c structures successively with their stable regions depending on the temperature and the shear rate. The a-b structure is composed of coexistent a and b structures. If the temperature is further lowered, precessional motions around the x axis are induced, leading to a_m, a_s, $a(b)$, and a_c structures with their precessional motions characterized by $n_y(t)^2/n_{y0}^2+n_z(t)^2/n_{z0}^2=1$. Here, $n_y(t)=n_{y0}\cos(\omega_0 t)$ and $n_z(t)=n_{z0}\sin(\omega_0 t)$ are components of the director $\mathbf{n}(t)=(n_x(t),n_y(t),n_z(t))$ precessing around the x axis with an angular frequency of $\omega_0=[\dot{\gamma}^2(-\alpha_2\alpha_3^R)/\gamma_1^2]^{1/2}$ [9]. Here $\dot{\gamma}$ is shear rate, α_3^R is the renormalized viscosity coefficient of α_3 including the effect of the S_A fluctuation [9,12], and $\gamma_1=\alpha_3-\alpha_2$. Each structure has the following precessional motion. a_m structure: anisotropic precession with larger amplitude in the y direction ($n_{y0}>n_{z0}$). a_s structure: isotropic precession with equal amplitude in the y and z directions ($n_{y0}=n_{z0}$). $a(b)$ structure: anisotropic preces-

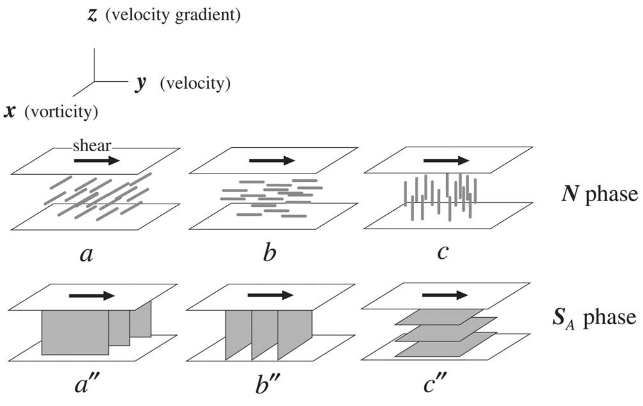

FIG. 1. Three fundamental structures in the nematic (N) phase under a shear flow along the y axis. a, b, and c structures have director orientations along vorticity (x), velocity (y), and velocity gradient (z) directions, respectively. In the S_A phase, additional layering is formed with its normal along the director orientation. The layer structures in this phase, a'', b'', and c'', are shown. In these structures, the directors are not depicted to avoid complexity.

sion with larger amplitude in the z direction ($n_{y0} < n_{z0}$). a_c structure: anisotropic precession with its motion largely deflected along the z axis ($n_{y0} \ll n_{z0}$). In the S_A phase, the formation of the layer structure makes the precessional motion impossible. In a temperature region just below the S_A-N phase transition point, a'' structure is induced, which at lower temperatures transforms to a''-c'' structure characterized by coexistent a'' and c'' structures. In the a''-c'' structure region, if the shear rate is increased it transforms to a'' structure at a critical shear rate with its transformation dependent on temperature; the critical shear rate becomes higher at lower temperatures.

For the behaviors when $\alpha_2/\alpha_3 < 0$ in the N phase, various studies have been made. In our rheological study of 8CB [13], it is suggested that the viscosity shows characteristic temperature dependence reflecting the above-mentioned shear-induced structures. Some other experimental [3,14–18] and theoretical [7,8,12,19,20] studies have shown that tumbling motion of the director occurs instead of the flow alignment of the director.

As for the shear-induced structural change in the S_A phase, the following results are obtained from rheological measurements performed by us [13] and Panizza *et al.* [21]. (1) When lowering the temperature from the S_A-N phase transition point, the low viscosity a'' structure changes to the high viscosity a''-c'' structure. (2) If the shear rate (shear stress) is increased in the a''-c'' structure region, the a''-c'' structure changes to the a'' structure above a critical shear rate (shear stress), accompanied by a change in the fluidity from non-Newtonian to Newtonian. Although the mechanism of the transformation from the a''-c'' to the a'' structure is not well clarified, theoretical studies on thermotropic smectics [22,23] and on lyotropic liquid crystals and block copolymers [24–26] may be suggestive; it is indicated that undulation instability plays a key role for the shear-induced structural change in the liquid crystals having lamellar structures.

As described above, some natures of the shear-induced structural changes in the N and the S_A phases are still unresolved. In the present study, dielectric properties under steady shear flow are measured in the N and the S_A phases of 8CB to make clear the relationships between the dielectric properties and the shear-induced structures and the mechanisms of the shear-induced structural changes in these phases.

II. EXPERIMENTAL

The liquid crystalline specimen 8CB was obtained from Merck Co. and was used without further purification. Varying the shear rate, rheological, and dielectric properties were measured simultaneously with a concentric cylinder viscometer without giving boundary condition (anchoring treatment) on the surfaces of the cylinders. For the measurements of the shear modified dielectric permittivity and loss, a small voltage (5 V) from an oscillator (FC110, YEW, Japan) was applied to the gap (1 mm) between the inner and outer cylinders, and the current passing through the specimen was phase-sensitively detected with a lock-in amplifier (LI5640, NF, Japan). Owing to this geometry, dielectric constants measured in this study are those along the velocity gradient direction. Except for the measurements of frequency dependence, dielectric measurements were made at 1 kHz. The temperature of the specimen was controlled with a precision of 0.05 K, using a temperature controller (340, Lakeshore, USA) and heater and thermocouple attached to the outer cylinder. The S_A-N and the N-I phase transition points were determined to be $T_{\mathrm{AN}}=306.3$ K and $T_{\mathrm{NI}}=313.7$ K, respectively, from the viscosity and dielectric measurements. With respect to the measurements of the dielectric constants (conductivity) under shear flow, the following pioneering works have been made. The dielectric permittivity under shear flow (flow-modified permittivity=FMP) was measured in suspension by Block *et al.* [27] to give evidence for the particle rotation under shear flow, and Panizza *et al.* [28] proposed a method to measure shear-modified conductivities along three directions (velocity, velocity gradient, and vorticity) for understanding of the shear-induced structures in lyotropic liquid crystals.

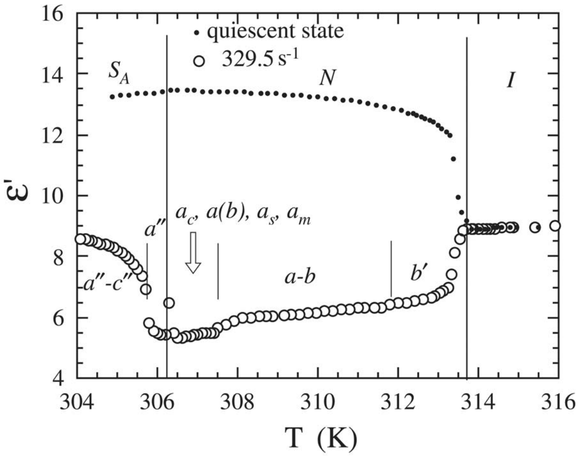

FIG. 2. Temperature dependence of dielectric permittivities in the quiescent state and under shear flow ($\dot{\gamma}=329.5\ \mathrm{s}^{-1}$). The dielectric permittivity is largely modified if the shear flow is applied, reflecting the shear-induced structures in the N and S_A phases.

III. RESULTS AND DISCUSSION

A. Temperature dependence

Temperature dependence of the dielectric permittivity ε' measured in the quiescent state and under steady shear flow ($\dot{\gamma}=329.5\ s^{-1}$) is depicted in Fig. 2. If lowering the temperature the dielectric permittivity in the quiescent state shows an abrupt increase just below the N-I phase transition T_{NI} point, followed by a gradual increase in the N phase and a change in the temperature coefficient at T_{AN}. This behavior is similar to $\varepsilon'_{\parallel}$ (dielectric permittivity along the optical axis of the director) [29], indicating that in the quiescent state the c structure is established in the N phase and the c'' structure in the S_A phases, with the director aligned along the velocity gradient direction (z axis). If a steady shear flow is applied, the dielectric permittivity is dramatically modified; ε' becomes lower in the N and S_A phases and shows characteristic temperature dependence which is absent in the quiescent

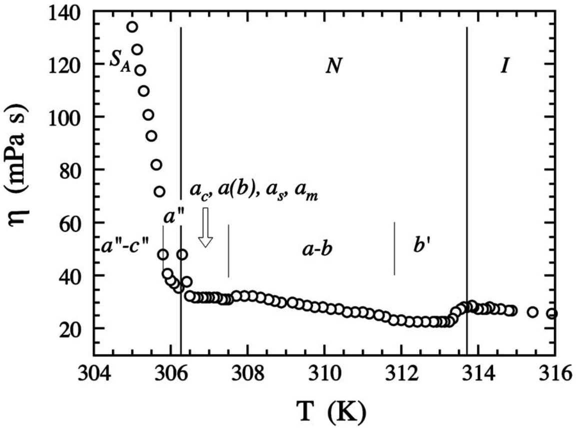

FIG. 3. Temperature dependence of viscosity measured at a shear rate of 329.5 s^{-1}. Like the dielectric permittivity (Fig. 2), the viscosity shows characteristic temperature dependence caused by the shear-induced structural changes.

state. It should be noted that such a behavior under a shear flow is reproducible even if the measurements are made repeatedly. To understand the relationship between the dielectric permittivity and the viscosity, the temperature dependence of the viscosity, which was obtained simultaneously with the dielectric permittivity, is given in Fig. 3. Furthermore, focusing on the temperature region near the S_A-N phase transition point, temperature dependence of both the dielectric permittivity and the viscosity is plotted in Fig. 4. In these figures, temperature regions of respective phases and the structures are specified by vertical lines. The results have the following characteristics when lowering the temperature from the I phase. (1) I phase: ε' is not modified by applying the shear flow, which can be understood if we consider the absence of the long-range orientational order in this phase. (2) Flow alignment b' region: Both ε' and η decrease with their temperature dependence larger near T_{NI}. These behaviors are similar to those of 5CB [4,30] exhibiting a flow alignment in the whole temperature region of the N phase. At the b' to a-b transition point, ε' decreases discontinuously and η changes its temperature coefficient. (3) a-b region: ε' decreases almost linearly, which is in contrast to the linear increase in η. Near the a-b to a_m transition point these quantities decrease critically. For understanding of the shear-induced structure in this temperature region, η is more useful than ε'. Since $\eta_a > \eta_b$, this gives us information about the fraction of the a and the b structures, whereas $\varepsilon'_a = \varepsilon'_b$, not giving such information. The temperature dependence of η in this region may suggest that the fraction of the b structure decreases with decreasing temperature toward T_{AN}. The b structure accompanied by the S_A fluctuation, i.e., short-range layer structure with its normal along the flow direction, is an unfavorable structure when the shear flow is applied along y axis [31]. Such kind of fluctuation is gradually developed when lowering the temperature to T_{AN}, which may cause the decrease in the fraction of the b structure. Although the details of the a-b structure are not given in the x-ray study [9], some structures are suggested from other studies; tumbling in the shear plane ($n_x=0, n_y \neq 0, n_z \neq 0$) [16], a structure ($n_x \neq 0, n_y=0, n_z=0$) [18], and twisted structure (xy plane) developed along the z axis ($n_x \neq 0, n_y \neq 0, n_z=0$) [20]. Our result can be consistently interpreted if we consider that the a-b structure corresponds to the twisted structure. (4) a_m region: A slight decrease is observed in ε' while a slight increase in η. The magnitude of η is somewhat larger than the literature value of η_a [31], indicating that the precessional motion of the director contributes to this increment of the viscosity. At the a_m to a_s transition point, the temperature coefficient of ε' becomes larger whereas there is no change in η. (5) a_s and $a(b)$ regions: ε' becomes lower while η shows small temperature dependence. The anomaly due to a_s to $a(b)$ structural change is not confirmed in ε' and η, indicating that the difference in the structure between the a_s and $a(b)$ structures, even if these structures are formed in this region, is small. At the $a(b)$ to a_c transition point ε' and η increase steeply. (6) a_c region. ε' and η have larger values accompanied by peaks, which can be reasonably understood in terms of the precessional motion of this structure; the precession is largely deflected along the z axis ($n_z \gg n_y$). In 8CB, ε'_c (η_c) is larger than ε'_a and ε'_b (η_a and η_b) [29,31], indicating that if n_z is larger than n_x and n_y, ε' and η become larger. (7) a'' region: ε' and η slightly increase with ε' having smaller temperature dependence than that of η. ε' in this region is almost the same with that in the precession region, implying that the director is aligned along the x axis. η in this region is larger than that in the precession region, suggesting that the interlayer interaction in the S_A phase contributes to this increment of the viscosity. (8) a''-c'' region. Both ε' and η increase steeply accompanied by a saturation of ε' and a continuous increase in η at lower temperatures. The behavior of ε' suggests that the fraction of the c'' structure increases and saturates around 304 K. The c'' structure thus developed coexists with the a'' structure, forming a complex structure responsible for the high viscosity. How the a'' structure coexists with the c'' structure will be discussed later. In such a way, the observed temperature dependence of the dielectric constants and the viscosity is almost consistently interpreted based on the shear-induced structures suggested by the x-ray study [9].

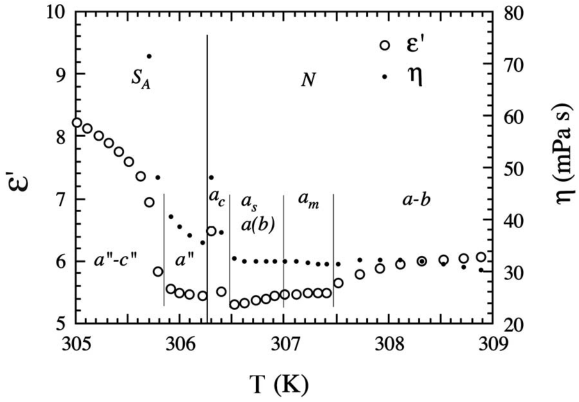

FIG. 4. Temperature dependence of the dielectric permittivity and the viscosity near the S_A to N phase transition point T_{AN}. These behaviors are consistently interpreted in terms of the shear-induced structures suggested by the x-ray scattering (Ref. [9]).

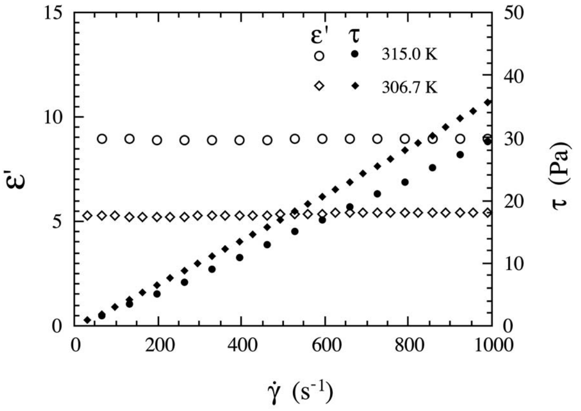

FIG. 5. Shear rate dependence of the dielectric permittivity and the shear stress in the I and the N phases. As representative data of the N phase, those at 306.7 K are given, since similar results were obtained in other temperature regions except for a_c region, where the measurements were not successful owing to large scatter of the data. In the I phase and a-b, a_m, a_s, and $a(b)$ regions of the N phase, the flow is Newtonian and the dielectric permittivity is not dependent on the shear rate.

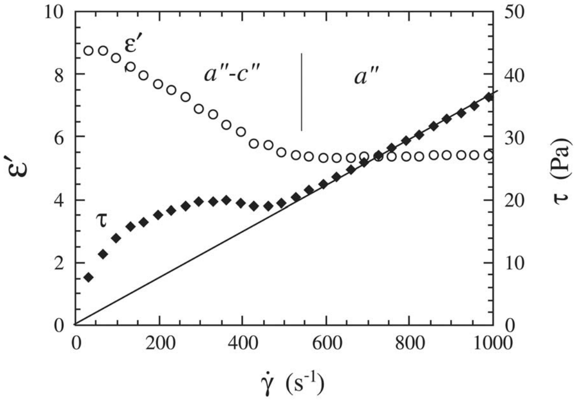

FIG. 6. Shear rate dependence of the dielectric permittivity and the shear stress in the S_A phase (305.9 K). With increase in the shear rate, the a''-c'' structure changes to the a'' structure accompanied by a change in flow from non-Newtonian to Newtonian and a decrease in the dielectric permittivity. The solid line is given to show the Newtonian behavior at higher shear rates. The dielectric behavior indicates that the fraction of c'' structure in the a''-c'' structure decreases in the course of this structural change.

B. Shear rate dependence

Shear rate dependence of the dielectric permittivity ε' and the shear stress τ in the I and the N phases is plotted in Fig. 5. As representative results of the N phase, those at 306.7 K [a_s and $a(b)$ regions] are given, since the shear rate dependence of ε' and τ in the a-b, a_m, a_s, and $a(b)$ regions shows similar behaviors. In the a_c region reproducible data were not obtained owing to a large scatter of the data. As this figure shows, in the I phase the shear stress increases linearly with the shear rate (Newtonian flow) and the dielectric permittivity is almost constant without depending on the shear rate, which can be easily expected if we consider the disordered nature of the I phase. As described above, in the N phase some complex structures appear, making us expect appearance of some complex fluidity, however, the results are similar to those in the N phase. These facts indicate that in the N phase the change in the shear rate does not affect the shear-induced mixed and the precessional structures.

In Fig. 6, results in the a''-c'' region (305.9 K) of the S_A phase are given. As clearly seen in this figure, the shear stress increases nonlinearly with the shear rate (non-Newtonian flow) in the lower shear rate region, but increases linearly (Newtonian flow) above a critical shear rate $\dot{\gamma}_c$. Such a change in the rheology can be attributed to the shear-induced structural change from the a''-c'' to the a'' structure as has been reported [9]. In the dielectric permittivity, a critical change, which is consistent with the rheological change, is observed. With increase in the shear rate, the dielectric permittivity gradually decreases, and above $\dot{\gamma}_c$ it becomes almost constant. This result indicates that with increasing the shear rate the fraction of the c'' structure component in the a''-c'' structure decreases, i.e., the anisotropy of the a''-c'' structure increases in the course of the a''-c'' to a'' structural change. With respect to the a''-c'' structure, x-ray scattering performed under a steady shear flow suggests that it is composed of multilamellar cylinders oriented along the velocity direction (y axis) with the long axis of the cylinders isotropically dispersed in the x-z plane [21]. However, the fact that the anisotropy of the a''-c'' structure increases with the shear rate may not be compatible with this kind of isotropically arranged cylindrical structure. Another possible structure for the a''-c'' structure should be considered, which will be discussed in the next section.

C. Frequency dependence

Frequency dependence of the dielectric constants measured under a shear rate of 329.5 s^{-1} in the I and the N

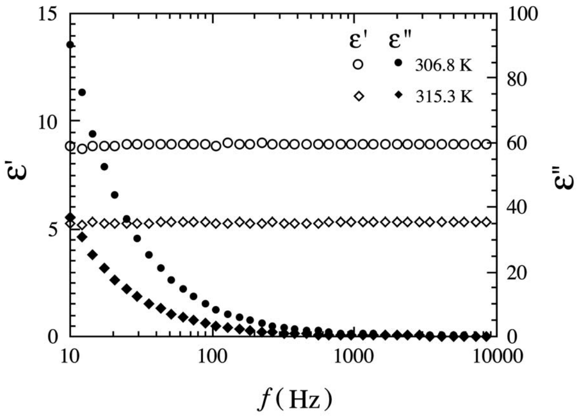

FIG. 7. Frequency dependence of the dielectric permittivity and loss under a shear flow ($\dot{\gamma}$=329.5 s^{-1}) in the I and N phases. As representative data of the N phase, those at 306.8 K are given, since similar results were obtained in other temperature regions except for the a_c region, where the measurements were not successful owing to large scatter of the data. In these phases, no dielectric dispersion is observed. The large dielectric losses at lower temperatures are due to dc conductivity.

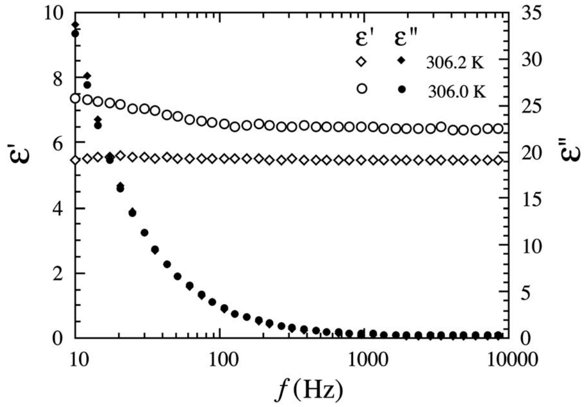

FIG. 8. Frequency dependence of the dielectric permittivity and loss under a shear flow ($\dot{\gamma}=329.5\ \mathrm{s}^{-1}$) in the S_A phase. In the a'' region (306.2 K), the dielectric dispersion is not observed like I and N phases, while in the a''-c'' region (306.0 K) it is observed at lower frequencies. The relaxation time of this shear-excited mode is ~4 msec.

phases is given in Fig. 7. As representative data of the N phase, those at 306.8 K [a_s and $a(b)$ regions] are given, since the spectra for the shear-induced structures, a-b, a_m, a_s, and $a(b)$, in the N phase resemble each other. The measurement in the a_c region was not successful owing to a large scatter of the data. In the I phase, the dielectric permittivity ε' is not dependent on the frequency, while the dielectric loss ε'' increases at lower frequencies. This increase in ε'' at lower frequencies is due to dc conductivity (σ), which contributes to ε' as σ/ω. The results in the N phase are similar to those in the I phase, only modified in the magnitude of ε'' at lower frequencies. The dielectric spectrum under the shear flow in the I and the N phases, thus shows no dielectric dispersion. In Fig. 8, results in the S_A phase are given. At 306.2 K (a'' structure region), the behaviors of ε' and ε'' are similar to those in the I and the N phases without showing dielectric dispersion. While at 306.0 K (a''-c'' structure region), a dielectric dispersion appears in ε'. Although the dielectric dispersion is not confirmed in ε'', if the contribution from the dc conductivity, σ/ω, is subtracted from the observed ε'', a peak centered around 40 Hz is obtained. These results indicate that the dielectric dispersion is caused by a shear-excited mode having a relaxation time of ~4 msec. Considering that the dielectric dispersion disappears in the course of the a''-c'' to a'' structural change, it is plausible to expect that the shear-excited mode has a key role in this structural change. For identification of this mode, recent theoretical studies for the shear-induced structural change in the lamellar system are suggestive [24–26]. It is indicated that if a steady shear flow along the y axis is applied to the c'' structure and the shear rate is increased, it changes to the a'' structure via a formation of an undulation. The undulation thus formed is suggested to have a displacement of the layer along the z axis and a wave vector along the x axis as shown in Fig. 9. In such an undulation, the director has components of ($n_x \neq 0$, $n_y=0$, $n_z \neq 0$), which may be compatible with the a''-c'' structure suggested by the x-ray study and also consistently explains our dielectric results. Furthermore, it has been known that the relaxation time of the undulation is of order of msec [2], which is compatible with our observed relaxation time. The presence of the undulation is also supported by the theoretical work by Goulian and Milner [22], which indicates that in the sheared smectics the undulation instability of the c'' structure leads to the a'' structure. Although further studies are necessary, it is possible to suggest that the a''-c'' structure is characterized by an undulation and the shear-induced structural change from the a''-c'' to the a'' structure occurs via the undulation instability.

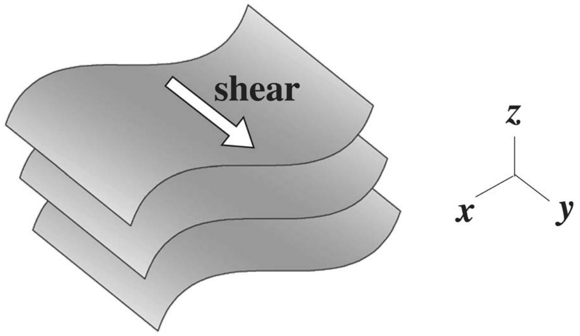

FIG. 9. Schematic drawing of the undulation in the a''-c'' structure. It is expected that the steady shear flow along the y axis induces undulation with the layer displacement along the z axis and the wave vector along the x axis to give the a''-c'' structure.

IV. SUMMARY

Dielectric permittivities under steady shear flow and rheological properties are measured to investigate the shear-induced structural changes in the N and the S_A phases of 8CB. The results are almost consistent with the shear-induced structures determined by x-ray scattering method. In the N phase, characteristic behaviors are observed in the temperature dependence of the dielectric permittivity and the viscosity, showing the existence of the successive structural changes caused by the development of the fluctuation of the S_A order. In the S_A phase, the shear induced structural change from the a''-c'' to the a'' structure is evidenced in the rheological and dielectric properties and as a possible mechanism of this shear-induced structural change undulation instability is suggested. The present study has clarified some unknown features of the shear-induced structures of the liquid crystals having a phase sequence of Cry-S_A-N-I, but further studies are necessary to understand the behaviors more definitively. If the precession of the director occurs in the N phase, its motion can be detected as a resonance peak in the dielectric spectrum such as the colloidal suspension [27,32], where the shear-induced particle rotation gives rise to a resonance peak in the spectrum of the dielectric permittivity. The quantitative characterization of the shear-induced structural change in the S_A phase is also necessary. Focusing on these unresolved natures, further studies are in progress.

[1] P. G. de Gennes and J. Prost, *The Physics of Liquid Crystals*, 2nd edition (Oxford University Press, 1993).
[2] S. Chandrasekhar, *Liquid Crystals*, 2nd edition (Cambridge University Press, 1992).
[3] Ch. Gähwiller, Phys. Rev. Lett. **28**, 1554 (1972).
[4] K. Negita, J. Chem. Phys. **105**, 7837 (1996).
[5] F. M. Leslie, Q. J. Mech. Appl. Math. **19**, 357 (1966).
[6] J. L. Ericksen, Arch. Ration. Mech. Anal. **4**, 231 (1960).
[7] T. Carlsson, Mol. Cryst. Liq. Cryst. **104**, 307 (1984).
[8] T. Carlsson and K. Skarp, Mol. Cryst. Liq. Cryst. **78**, 157 (1981).
[9] C. R. Safinya, E. B. Sirota, and R. J. Plano, Phys. Rev. Lett. **66**, 1986 (1991).
[10] C. R. Safinya, E. B. Sirota, R. Plano, and R. F. Bruinsma, J. Phys.: Condens. Matter **2**, SA365 (1990).
[11] K. Skarp, T. Carlsson, S. T. Lagerwall, and B. Stebler, Mol. Cryst. Liq. Cryst. **66**, 199 (1981).
[12] R. F. Bruinsma and C. R. Safinya, Phys. Rev. A **43**, 5377 (1991).
[13] K. Negita and S. Uchino, Mol. Cryst. Liq. Cryst. Sci. Technol., Sect. A **378**, 103 (2002).
[14] P. Pieranski and E. Guyon, Phys. Rev. Lett. **32**, 924 (1974).
[15] P. E. Cladis and S. Torza, Phys. Rev. Lett. **35**, 1283 (1975).
[16] T. Carlsson and K. Skarp, Liq. Cryst. **1**, 455 (1986).
[17] P. T. Mather, D. S. Pearson, and R. G. Larson, Liq. Cryst. **20**, 539 (1996).
[18] D. Gu and A. M. Jamiesen, J. Rheol. **38**, 555 (1994).
[19] G. Marrucci, Macromolecules **24**, 4176 (1991).
[20] W. H. Han and A. D. Rey, J. Rheol. **39**, 301 (1995).
[21] P. Panizza, P. Archambault, and D. Roux, J. Phys. II **5**, 303 (1995).
[22] M. Goulian and S. T. Milner, Phys. Rev. Lett. **74**, 1775 (1995).
[23] R. Bruinsma and Y. Rabin, Phys. Rev. A **45**, 994 (1992).
[24] A. G. Zilman and R. Granek, Eur. Phys. J. B **11**, 593 (1999).
[25] G. K. Auernhammer, H. R. Brand, and H. Pleiner, Phys. Rev. E **66**, 061707 (2002).
[26] Th. Soddemann, G. K. Auernhammer, H. Guo, B. Dünweg, and K. Kremer, Eur. Phys. J. B **13**, 141 (2004).
[27] H. Block, K. M. W. Goodwin, E. M. Gregson, and S. M. Walker, Nature (London) **275**, 633 (1978).
[28] P. Panizza, A. Colin, C. Coulon, and D. Roux, Eur. Phys. J. B **4**, 65 (1998); Phys. Rev. E **64**, 021502 (2001).
[29] J. Thoen and G. Menu, Mol. Cryst. Liq. Cryst. **97**, 163 (1983).
[30] K. Negita and C. Nishikawa, J. Chem. Phys. **125**, 144517 (2006).
[31] H. Kneppe, F. Schneider, and N. K. Sharma, Ber. Bunsenges. Phys. Chem. **85**, 784 (1981).
[32] Y. Misono and K. Negita, Phys. Rev. E **70**, 061412 (2004).